

## Depth dependence for extended x-ray-absorption fine-structure spectroscopy detected via electron yield in He and in vacuum

W. T. Elam, J. P. Kirkland,\* R. A. Neiser,\* and P. D. Wolf†

Condensed Matter Physics Branch, Condensed Matter and Radiation Science Division, Naval Research Laboratory, Washington, D.C. 20375-5000

(Received 12 February 1988)

X-ray absorption spectra have been measured using electron detection with both vacuum and helium gas surrounding the samples. The samples consisted of thin iron films covered with various thicknesses of aluminum to determine the contribution versus depth. The height of the iron  $K$ -absorption-edge jump decreases exponentially with aluminum covering thickness, with a  $1/e$  depth of 1600 Å. The addition of helium gas forms an ionization detector for the electrons, which have an average energy of about 2500 eV. The effects of electrode geometry and bias voltage are evaluated. When operated in a linear-response region, the signal-to-noise ratio for this method is excellent and the extended x-ray-absorption fine-structure (EXAFS) amplitudes agree with transmission measurements to better than 3%.

### INTRODUCTION

Since Kordesch and Hoffman<sup>1</sup> first used a detector inspired by conversion-electron Mössbauer spectroscopy to measure near-surface extended x-ray-absorption fine-structure (EXAFS) in bulk samples via electron yield, the technique has become increasingly popular.<sup>2,3</sup> It is simple, does not require vacuum or other elaborate apparatus, and allows examination of thin films as well as modified surfaces of bulk samples. It has high sensitivity and avoids the usual corrections for self-absorption necessary when using fluorescence detection for thick concentrated samples.

The principal limitation thus far has been limited knowledge of the precise depth dependence of the signal, in spite of much available literature on the transport of electrons in solid materials. The work most directly applicable to this technique is that motivated by conversion-electron Mössbauer spectroscopy. However, the results of this work can be difficult to interpret and in some cases yield contradictory quantitative information. The present experiments were undertaken to make empirical, quantitative measurements of EXAFS signals versus depth under a variety of commonly employed conditions. These measurements could then be used to select an appropriate model for interpreting measurements on unknown systems. In particular, this work was motivated by ambiguities in measurements of ion-implanted samples. The results have proven both the applicability of the technique and the reliability of the interpretations.

Figure 1 shows a simplified schematic of the processes which occur inside an iron sample during x-ray absorption. The incident x ray is stopped by an iron  $K$ -shell electron (at x-ray energies just above the iron  $K$  absorption edge) and produces an excited iron atom and a photoelectron. Near the absorption edge, the photoelectron has little energy and therefore only a short range. The excited atom can decay either by emitting a characteristic

x ray or by emitting Auger electrons. In conventional fluorescence EXAFS, the characteristic x rays are detected. Since the decay event is delayed in time by the core hole lifetime, it is independent of the details of the excitation process. Thus, for a fixed detector geometry, the decay products serve as a reliable monitor of the amount of incident x rays being absorbed.

The Auger electrons can also be detected. By placing an electrode (such as a grid or wire) in front of the sample, placing a bias voltage on the electrode, and measuring the current between this electrode and the sample (the sample current), a signal from the electrons emitted by the sample is obtained. This sample current (denoted  $I$  in the figure) will consist of both  $K$  and  $L$  Auger elec-

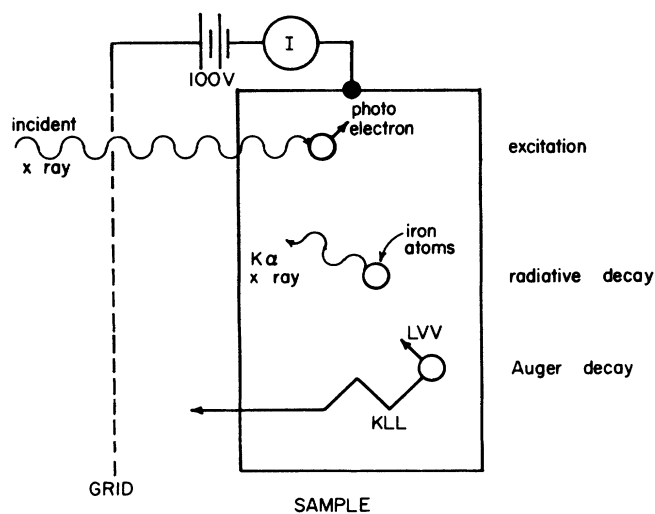


FIG. 1. Schematic of apparatus for electron detection of x-ray absorption spectra. Events in the sample leading to the production and escape of electrons and the method for measuring the electron yield (as a current,  $I$ ) are illustrated.

trons as well as photoelectrons and electrons excited by the emerging Auger electrons (referred to here as secondary electrons). Herein we report several measurements of the magnitude of this sample current as a function of incident x-ray flux and energy for several measurement conditions. The dependence on depth within the sample and the effect of adding helium gas to make a simple flow detector have been particularly emphasized.

### EXPERIMENT

The experiments were performed on the Naval Research Laboratory Materials Analysis Beamline (X23B) at the National Synchrotron Light Source. A focused, monochromatic x-ray beam was passed through a partially-transparent ionization chamber to provide incident beam normalization and then allowed to strike a sample placed at  $45^\circ$  to the beam axis. The apparatus is shown in Fig. 2. A large area ionization chamber<sup>4</sup> was placed at  $90^\circ$  to the x-ray beam and used to collect the usual fluorescence EXAFS signal. In addition, the sample current was amplified and recorded. A 90% transmission Ni mesh was placed about 1 cm from the sample biased at +100 V.

The measurements were made in a stainless steel chamber with 3-mil Kapton<sup>®</sup> windows to allow x rays in and out. The chamber was connected to a diffusion pump system and could be evacuated to less than  $10^{-5}$  Torr. The chamber could also be backfilled with commercial grade helium gas for comparison with the simple gas flow detectors. Both fluorescence x-ray and sample current signals were collected for a sequence of incident x-ray energies in the usual fashion of EXAFS measurements.

The samples were prepared for this experiment by evaporating 100 Å of iron onto a glass substrate. The iron was then covered with aluminum of various thicknesses. The thinnest Al overlayer was greater than 100 Å to in-

sure continuous coverage, and the thicknesses extended up to 6000 Å. Both iron and aluminum thicknesses were checked by x-ray fluorescence in a commercial spectrometer. The EXAFS data were obtained using x-ray energies around 7111 eV, the iron K absorption edge. A typical spectrum is shown in Fig. 3. The plot is sample current (normalized by the incident beam signal) versus incident photon energy. This sample is 100 Å of iron covered by 140 Å of aluminum. The chamber was evacuated to less than  $10^{-5}$  Torr for this spectrum, which is a single scan taken in less than 10 min.

The change in the normalized signal across the absorption edge was taken to be the signal amplitude for calculating the electron yields. The data below the edge was fit by least squares to a line, which was subtracted from the data. A short region of the signal above the edge was also fit to a line, which is shown in Fig. 3 superimposed on the data just at the top of the absorption edge. The value of this line at the edge energy of 7111 eV was used directly as the signal amplitude.

### ANALYSIS AND RESULTS

The most striking feature of the data obtained in vacuum by this method is the signal-to-noise ratio. In spite of the small sample currents involved (a few times  $10^{-11}$  amps), the spectrum is comparable to those taken on iron foils via transmission EXAFS, even though the sample is only 100 Å thick. The size of the iron edge jump decreases as the aluminum overlayer is made thicker, and is undetectable for 6000 Å of aluminum.

From the data in vacuum the detection efficiency (number of electrons per photon) and its dependence on depth within the sample can be calculated. Comparing the yield in helium with the yield in vacuum gives a measure of the gain provided by using the helium as an ionization detector for the electron yield. The average ener-

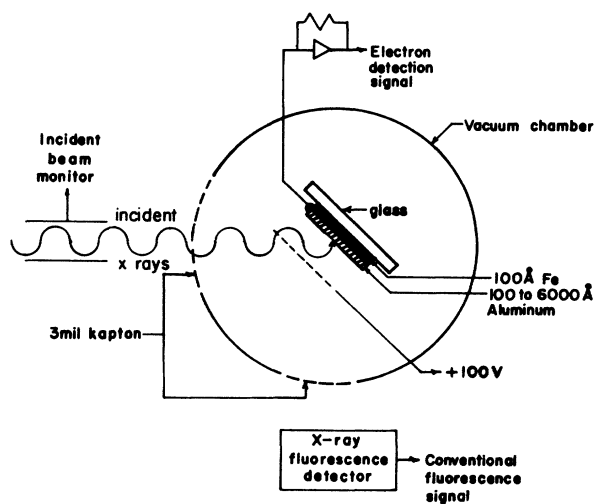


FIG. 2. Apparatus used to measure simultaneous fluorescence and electron EXAFS. Chamber could be evacuated to below  $10^{-5}$  Torr and backfilled with helium.

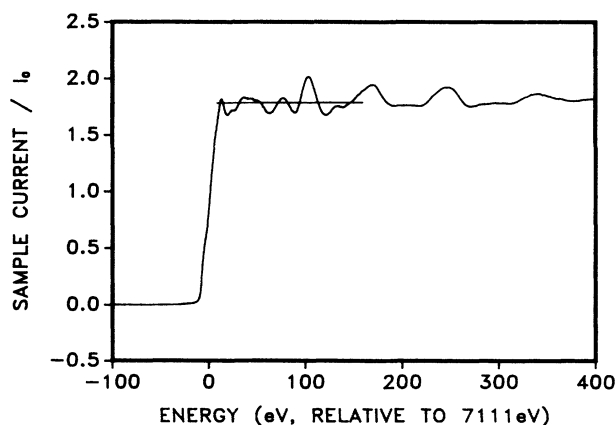


FIG. 3. Plot of sample current (normalized to incident beam monitor,  $I_0$ ) vs photon energy near the iron K absorption edge. The sample is a 100 Å film of iron on glass covered by a 140 Å layer of aluminum. The chamber was evacuated to below  $10^{-5}$  Torr. A linear pre-edge background has been subtracted from the data, and the short line superimposed just above the edge shows the fit used to determine the height of the edge step. The data are from a single scan taken in approximately 10 min.

gy to create an ion pair in helium can then be used to calculate the average electron energy.

The detection efficiency is obtained by converting the sample current into electrons per second and then dividing by the number of photons incident on the sample. The incident flux is found by converting the incident beam ion chamber current into photons absorbed in the detector, dividing by the absorption in the detector, and correcting for the air path and chamber windows. The energy dependence of the absorption coefficients as well as the absorption in the aluminum layer (maximum about 1%) were ignored. This information was used, together with amplifier gains, etc., to compute a factor relating the ratio of sample current to incident beam detector current (as obtained from Fig. 3) to the actual electrons per photon incident. The amplitude of the signal change across the edge was then found, corrected for the actual iron layer thickness, divided by the absorption in the iron layer, and multiplied by the above conversion factor. The results, as electrons per photon absorbed in a 100 Å iron layer, are presented in column 2 of Table I. As can be seen, the yields are of the order of one electron per absorbed photon, which accounts for the high signal-to-noise ratio.

The third column in the table gives the ratio of the signal in vacuum to that obtained when the chamber is filled with helium. Under these conditions, the system acts as an ionization chamber for detection of the electrons emitted from the sample, with the sample itself and the grid as electrodes. Reversing the grid bias reversed the polarity of the signal but had less than a 10% effect on the amplitude. The current is linear with respect to incident flux and independent of bias above some threshold value, typically a few volts at these low currents. Electrode geometries which produced nonuniform electric fields in the region near the sample surface also gave nonlinearity problems. For this reason, either a grid or an aluminized Mylar sheet is preferred as the bias electrode. Nonlinearity of the detector will seriously degrade the signal-to-noise ratio in EXAFS spectra because the fluctuations in intensity inherent in synchrotron sources will not be completely removed by normalization to the incident beam signal.

TABLE I. Electron yield per photon absorbed in a 100 Å film of iron covered by various amounts of aluminum. The electron yield is calculated from the change in total sample current as the x-ray energy is increased across the iron *K* absorption edge.

Aluminum thickness (Å)	Electrons per photon absorbed in 100 Å of iron (vacuum)	Ratio of He-to-vacuum
140	0.71	81
200	0.60	85
500	0.46	90
1100	0.38	82
2200	0.17	68
6100		

If one assumes that the electron emission from the sample surface is unaffected by the addition of helium gas, the average electron energy can be found by multiplying the ratio of helium-to-vacuum currents by the energy to create an ion pair in helium (denoted as  $W$ ). Since commercial helium is often contaminated with small amounts of argon<sup>5</sup> (about 0.1%), a value of  $W = 30$  eV was used, which is slightly smaller than the value for pure helium.<sup>6</sup> This value of  $W$  gives an average electron energy of about 2500 eV.

Figure 4 shows a plot of the log of the yield versus thickness of the aluminum overlayer. The dashed line has a slope of one over 1639 Å. Except for the thinnest overlayer, this simple exponential model fits the data acceptably well. Error bars are not shown, since the statistical measurement errors are very small (much less than 1%), but systematic errors in the various correction factors and in the thickness measurements are probably a few percent. The ratio of helium-to-vacuum signals should not be susceptible to these systematic errors, and should therefore be more precise (again, better than 1%). Detailed comparison of the EXAFS amplitudes using Fourier transforms and the ratio method indicates that the data collected in vacuum and in helium agree in detail as a function of energy to within 1%. They show about a  $3 \pm 2\%$  increase in first shell amplitude (when corrected for the energy dependence of the incident beam monitor) and an increase in radial distance of 0.4 Å when compared to an iron foil measured via transmission. Changes in the near-edge structure and the higher shell EXAFS indicate that there is some oxidation of the iron layer. The above figures thus provide an upper limit for any discrepancy between electron detection and transmission EXAFS.<sup>7</sup> The fluorescence data is noisier, but it agrees with both the transmission and electron data to within statistical error.

## DISCUSSION

The value for the average energy of the electrons is surprisingly high. One might expect that the cascade of

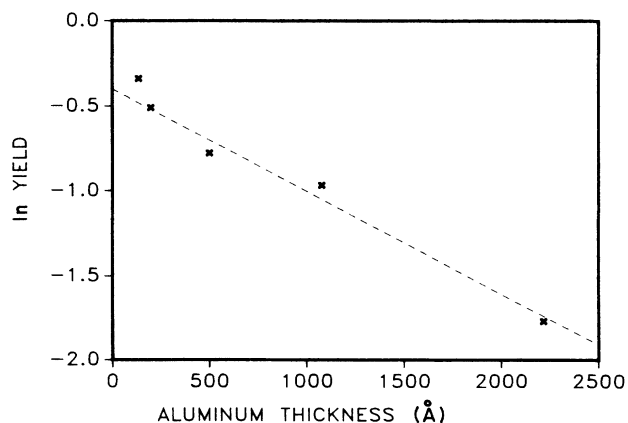


FIG. 4. Log of the electron per photon yield from Table I plotted vs aluminum overlayer thickness. The dashed line has a slope of 1 over 1639 Å. Errors are a few percent and are primarily in the iron and aluminum thickness measurements.

much lower energy (below 100 eV) secondary electrons would dominate. For the depths studied here, these lower energy electrons apparently do not escape. Only those electrons which retain an appreciable fraction of their original energy can escape and contribute to the signal. Spijkerman<sup>8</sup> has measured the detailed energy dependence of the emitted electrons in conversion electron Mössbauer spectroscopy for on- and off-resonance conditions. Both conditions have a large low-energy tail, but the signal from the on-resonance condition, corresponding to above the absorption edge in this work, has a broad energy distribution from about 1 to 5 keV. The average energy value from this work is consistent with such a distribution, although the detailed energy dependence was not measured. The initial rise in the helium-to-vacuum ratio versus depth (column 3 of Table I) together with the increased yield for the thinnest overlayer indicate that more low-energy (Auger and secondary) electrons escape through the thinner layers. The ultimate fall in this ratio with increasing thickness is due to increased energy loss of the escaping higher-energy Auger electrons.

Both the exponential depth dependence and the high average energy are consistent with the "diffusion" regime described by Coslett and Thomas<sup>9</sup> for transmission of electrons through metal foils. In this regime, the escaping electrons have lost appreciable energy via many scattering events, losing a few eV in each event. Huffman<sup>10</sup> has applied their results to conversion-electron Mössbauer spectroscopy and his treatment is relevant to this work. His form of the results of Coslett and Thomas gives an escape depth of 1050 Å for Fe Auger electrons at 5.4 keV, somewhat shorter than the result obtained here. This may be due to extrapolation of the results of Coslett and Thomas to an energy range somewhat lower than their measurements. Kantor<sup>11</sup> has made measurements similar to those of Coslett and Thomas in an energy range more relevant to this work. He predicts the fraction transmitted above some critical energy, which gives numbers too large for the thinner layers of aluminum studied here. His results also predict values for the average energy of the emitted electrons which are almost a factor of 2 too large. More sophisticated calculations, based on Monte Carlo techniques, have been performed by Liljequist, Ekdahl, and Bäverstam<sup>12</sup> for conversion-electron Mössbauer spectroscopy. Their predictions are the most complete and relevant, as they give a quadratic form for the fraction of iron Auger electrons transmitted out of the sample as a function of depth. However, their results are not substantially better than the exponential form, and overestimate the contribution at large thicknesses. Their values for the average energy are also somewhat high.

Cargill<sup>13</sup> has performed experiments almost identical to those described here, and obtains almost identical numbers for the electron per photon yield. He has also proposed a model for electron escape which accounts for the increase in yield for thinner overlayers. His experiments involve higher energies, and the effect is more pronounced. Preliminary results from experiments of Shih and co-workers<sup>14</sup> on submonolayer BaO on tungsten

dispenser cathodes performed in ultrahigh vacuum indicate that the yields may be as much as 2 orders of magnitude higher. This high yield is presumably from the escaping low-energy cascade of secondary electrons produced by the Ba Auger electrons. It should be kept in mind that these are atoms on the outer surface of materials with an unusually low work function and designed for high electron emission. Experiments performed in helium gas should not show this enhanced surface sensitivity, since the low-energy electrons do not have enough energy to ionize the helium.

## CONCLUSIONS

For the range of thicknesses studied here, the dependence of electron yield on depth within the sample is adequately described by an exponential decay. The average energy of the escaping electrons is about 2500 eV and the escape depth is 1600 Å for the iron absorption edge and aluminum overlayers. Since the escape depth for electrons is relatively independent of material when expressed in mass per unit area,<sup>9,10,12</sup> an approximate value should be easily obtainable for most experiments. Using the equation in Huffman<sup>10</sup> based on the results of Coslett and Thomas,<sup>9</sup> and applying a numerical correction to agree with the present measurements gives

$$d = \frac{0.011}{\rho(\text{g/cm}^3)} [E(\text{eV})]^{3/2} \text{ \AA} ,$$

where yield  $\propto e^{-x/d}$  and  $d$  is the escape depth in angstroms,  $x$  is the depth from the sample surface,  $\rho$  is the density in grams per cubic centimeter, and  $E$  is the energy of the Auger electrons in eV. Kantor<sup>11</sup> finds that the correction for oxidation of the aluminum is about 3.6  $\mu\text{g/cm}^2$ . For depths less than about 100 Å of aluminum (2.7  $\mu\text{g/cm}^2$ ) at 5500 eV, sensitivities may be somewhat higher for experiments performed in vacuum and the simple exponential dependence may break down.

The yields and collection efficiencies are large, of the order of 1 electron per absorbed photon in thin layers. Use of helium gas as an ionization detector for the secondary electrons yields almost a factor of 100 increase in current, improving the immunity to electronic noise and allowing the use of simple flow detectors. Electrode geometry and bias are not critical provided a very uniform electric field is maintained.

## ACKNOWLEDGMENTS

The authors would like to thank many people for assistance in this work. We are especially indebted to B. Jonker and G. A. Prinz for preparing the samples. A. Shih allowed us to use his data prior to publication. Many of the ideas herein are from valuable and fruitful discussions with K. S. Grabowski, C. M. Dozier, C. E. Bouldin, B. A. Bunker, K. I. Pandya, R. W. Hoffman, and G. S. Cargill, III. D. B. Brown greatly improved the manuscript by his critical comments. The measurements were performed on National Synchrotron Light Source

(NSLS) X23B, the NRL Materials Analysis Beamline, designed and built by J. P. Kirkland and R. A. Neiser. This research was carried out (in part) at the National Synchrotron Light Source, Brookhaven National Labora-

tory (Upton, NY), which is sponsored by the U.S. Department of Energy (Division of Materials Science and Division of Chemical Sciences of the Office of Basic Energy Sciences), under Contract No. DE-AC02-76CH00016.

---

\*Also at Sachs/Freeman Associates, Inc., 1401 McCormick Drive, Landover, MD 20785-5396.

†Present address: Phillips Electronic Instruments, Mahwah, NJ 07430.

<sup>1</sup>M. E. Kordesch and R. W. Hoffman, *Phys. Rev. B* **29**, 491 (1984).

<sup>2</sup>C. E. Bouldin, R. A. Forman, and M. I. Bell, *Phys. Rev. B* **35**, 1429 (1987).

<sup>3</sup>F. W. Lytle, R. B. Greegor, G. H. Via, J. M. Brown, and G. Meitzner, *J. Phys. C* **8**, 149 (1986).

<sup>4</sup>E. A. Stern, W. T. Elam, B. A. Bunker, K. Lu, and S. M. Heald, *Nucl. Instrum. Methods* **195**, 345 (1982).

<sup>5</sup>J. E. Parks, G. S. Hurst, T. E. Stewart, and H. K. Weidner, *J. Chem. Phys.* **57**, 5467 (1972).

<sup>6</sup>International Commission on Radiation Units and Measurements Report No. 31, 1979 (unpublished).

<sup>7</sup>T. Guo and M. L. den Boer, *Phys. Rev. B* **31**, 6233 (1985).

<sup>8</sup>J. J. Spijkerman, *Mössbauer Effect Methodology* **7**, 85 (1971).

<sup>9</sup>V. E. Coslett and R. N. Thomas, *B. J. Appl. Phys.* **15**, 883 (1964).

<sup>10</sup>G. P. Huffman, *Nucl. Instrum. Methods* **137**, 267 (1976).

<sup>11</sup>H. Kanter, *Phys. Rev.* **121**, 461 (1961).

<sup>12</sup>D. Liljequist, T. Ekdahl, and U. Bäverstam, *Nucl. Instrum. Methods* **155**, 529 (1978).

<sup>13</sup>G. S. Cargill, III, A. Erbil, R. Frahm, and R. F. Boehme, *Bull. Am. Phys. Soc.* **32**, 508 (1987).

<sup>14</sup>A. Shih (private communication).